Proceedings of the
47th IEEE Conference on Decision and Control
Cancun, Mexico, Dec. 9-11, 2008

Decentralized Receding Horizon Control Using Communication Bandwidth Allocation

H. A. Izadi, *Student Member, IEEE,* B. W. Gordon, and C. A. Rabbath, *Senior Member, IEEE*

Abstract—**The decentralized receding horizon control (DRHC) of a team of cooperative vehicles with limited communication bandwidth is considered. It is well known that the more communication the better stability and performance properties of the cooperative vehicles; however, in reality the available communication is often limited. This motivates our research to develop a new algorithm for efficient usage of available communication capacity so that the teaming behavior is optimized. The proposed algorithm uses a bandwidth allocation method; the key idea is to reduce the overall mismatch between predicted and actual plans of each neighbor by efficient communication bandwidth allocation.** [1]

I. INTRODUCTION

The recent advances in distributed computation allow using optimization-based control methods such as receding horizon control (RHC) [1, 2], and decentralizing the control problems[3-5]. Such fact has motivated researchers to develop RHC based decentralized control architectures [1, 3-5] for cooperative multi-agent systems. However, proving stability and feasibility of DRHC-based cooperative control systems is still a challenge [3, 6-8] and hence remains an ongoing research area.

The stability and performance of DRHC-based cooperative control systems may be enhanced by modifying the cost function and constraints [3-8]. However, the communication based methods offer another potential method for improving the performance of DRHC in the context of cooperative control of multi-agents. This paper aims at improving the performance of DRHC by proposing a DRHC technique that includes allocating the available, although limited, communication resources to the different agents in the team. In this paper, bidirectional communication is assumed available to the neighboring vehicles; however, the bandwidth in the communication channels is limited. The latter is a practical consideration that may lead to delayed information exchanges among agents and, if not handled properly, may cause instability. The key idea in this paper is to enable the DRHC to allocate a greater portion of the available bandwidth to agents in need, with objective of maintaining fleet cohesion. However, one must define what qualifies as an agent in need. Further, one must determine the portion of the available communication bandwidth that should be used in critical situations. Such questions have motivated this paper.

Few works in the context of DRHC have addressed such questions. In [9], the problem of optimal formation control under limited communication capacity is considered for two-vehicle formations. They demonstrate that, in the case of noise-free communication, bit-limited exchanges can reduce the performance of the fleet by as much as 20% when compared to the case of unlimited communication capacity. In another work [10] the effect of limited communication bandwidth on the control of multiple miniature robots is studied and a bandwidth allocation algorithm is presented. However, the team control is accomplished in a centralized fashion, contrary to our work.

This paper is organized as follows. The DRHC problem is formulated in Section II. Each agent plans its own trajectory and predicts plan of its neighbors based on the dynamical model available. Section III and IV discuss the stability and performance analysis respectively. The results of Section III and IV indicate that the mismatch between the predicted and the actual trajectories of agents, labeled as *prediction mismatch* in this paper, has a significant influence on both stability and performance of DRHC-based cooperative control systems. Section V summarizes the results and presents the proposed algorithm. In Section VI, the proposed DRHC algorithm is applied to formation control of a team of vehicles with uncoupled dynamics and limited communication bandwidth.

II. PROBLEM FORMULATION

A. Interaction and Information Exchange Graphs

The interaction between cooperative vehicles is usually represented by an "*interaction graph*" including nodes and arcs. The nodes represent the vehicles and an arc between two nodes denotes a coupling term in the objectives and/or in the constraints associated to the nodes. Also, it is usually assumed that the *exchange of information* has a particular structure; in this paper it is assumed that the *information exchange graph* is fixed and that each vehicle can communicate information with only a subset of the other vehicles in the team. Furthermore, we assume the *interaction graph* and the *information exchange graph* coincide; that is, only the vehicles that have interaction with each other, such as in collision avoidance algorithms, will exchange information.

[1] Manuscript received March 1, 2008. H. Izadi and B. W. Gordon are with Department of Mechanical and Industrial Engineering, Concordia University, 1455 de Maisonneuve Blvd. West, Montreal, Quebec, H3G 1M8, Canada (e-mail: ha_izadi@encs.concordia.ca, bwgordon@encs.concordia.ca). C. A. Rabbath is with Defence R&D Canada – Valcartier, 2459 Pie-XI Blvd North, Quebec City, QC, G3J 1X5, Canada (e-mail: Camille-Alain.Rabbath@drdc-rddc.gc.ca).

978-1-4244-3124-3/08/$25.00 ©2008 IEEE

Considering a set of N_v vehicles cooperating to perform a common mission, the i^{th} vehicle corresponds to the i^{th} node of the graph. If an arc (i, j) connecting the i^{th} and j^{th} node is present, it means that the i^{th} and j^{th} vehicles have a coupling term in their cost function and/or in their constraints (interaction), and communicate with each other. This relationship is termed as a *neighborhood* for the i^{th} and j^{th} vehicles. This leads to the interaction graph:

$$G(t) = \{V, E\} \tag{1}$$

where V is the set of nodes (vehicles) and $E \subseteq V \times V$ the set of arcs (i,j), with $i, j \in V$. The interaction graph is indirect i.e. $(i, j) \in E$ implies $(j,i) \in E$ even though it does not appear in E. This graph topology enables us to represent all configurations of the subgroups in terms of interaction and information exchange graphs. For the remainder of the paper, let N_n^i denote the number of neighbors of vehicle i. Also, the terms "agent", "vehicle" and "team member" bear the same meaning.

B. DRHC formulation

With Receding Horizon Control (RHC) –also known as model predictive control- a cost function is optimized over a finite time called *prediction horizon* T, or in short *horizon*. The first portion of the computed optimal input is applied to the plant during a period of time called the *execution horizon*, δ, or *sampling period*. The reader is referred to [11] for a comprehensive review of RHC.

Let us assume that the *execution horizon* δ is equal to the *communication period.* We can thus suppose there is synchronization between the communication rate and the sampling rate of RHC. Then, let the following represent the concatenated state and input vectors of the neighbors of i^{th} vehicle at time t_k, where $t_{k+1} = t_k + \delta$ is the discrete time and $t_0 = 0$:

$$\begin{aligned} \hat{x}^i(t_k) &= [\ldots, x^j(t_k), \ldots]^T \quad ; j \in V,\ (i,j) \in E \\ \hat{u}^i(t_k) &= [\ldots, u^j(t_k), \ldots]^T \quad ; j \in V,\ (i,j) \in E \end{aligned} \tag{2}$$

where $x^i(t)$ and $u^i(t)$ are the state and the input vectors of the i^{th} vehicle, respectively, at time t. Also, let the following include the state and the input vectors of i^{th} vehicle and the concatenated vectors $\hat{x}^i(t_k)$ and $\hat{u}^i(t_k)$, respectively:

$$\begin{aligned} \tilde{x}^i(t_k) &= [x^i(t_k), \hat{x}^i(t_k)]^T \\ \tilde{u}^i(t_k) &= [u^i(t_k), \hat{x}^i(t_k)]^T \end{aligned} \tag{3}$$

vectors $\tilde{x}^i(t_k)$ and $\tilde{u}^i(t_k)$ represent the updated information available to the i^{th} vehicle at time t_k. The following represents the decentralized cost function for the i^{th} vehicle in the team at time t_k:

$$\begin{aligned} J_T^i(\tilde{x}^i(t_k), \tilde{u}^i(t_k)) &= L_T^i(x^i(t_k), u^i(t_k)) + \\ &\sum_{(i,j)\in E} [L_T^j(x^j(t_k), u^j(t_k)) + l_T^{i,j}(x^i(t_k), x^j(t_k))] \end{aligned} \tag{4}$$

where, the term $L_T^i(x^i(t_k), u^i(t_k))$ in (4) is associated to the cost of the individual vehicle i over the prediction horizon T. Also, the term $l_T^{i,j}(x^i(t_k), x^j(t_k))$ represents the *coupling cost* between i^{th} and j^{th} vehicles over $[t_k, t_k + T]$. As seen from (4) the decentralized cost function includes the cost associated to each vehicle and that of its neighboring vehicles, and not all the vehicles in the team.

Suppose that the following represents the nonlinear dynamics of the i^{th} vehicle:

$$\dot{x}^i(t) = f(x^i(t), u^i(t)), \quad f(0,0) = 0 \tag{5}$$

Assume $x_{t_k}^i(t)$ denotes the state vector of the i^{th} vehicle at time t, calculated by solving the optimization problem $P^i(t_k)$ at time t_k and also $x^i(t)$ denotes the actual state of i^{th} vehicle at time t. The DRHC problem $P^i(t_k)$ is then defined for the i^{th} vehicle at time t_k as follows:

DRHC Problem $P^i(t_k)$ *:*

$$\tilde{u}_{t_k}^i(\cdot) = \arg \mathrm{Min}\ J_T^i(\tilde{x}^i(t_k), \tilde{u}^i(t_k)) \tag{6}$$

Subject to:

$$\dot{x}_{t_k}^i(t) = f(x_{t_k}^i(t), u_{t_k}^i(t)); \tag{7a}$$

$$x_{t_k}^i(t_k) = x^i(t_k);\ t \in [t_k, t_k + T]$$

$$x_{t_k}^i(t) \in \mathrm{X}^i,\ u_{t_k}^i(t) \in \mathrm{U}^i;\ t \in [t_k, t_k + T] \tag{7b}$$

$$\dot{x}_{t_k}^j(t) = f(x_{t_k}^j(t), u_{t_k}^j(t)); \tag{7c}$$

$$x_{t_k}^j(t_k) = x^j(t_k); t \in [t_k, t_k + T];\ \ (i,j) \in E$$

$$x_{t_k}^j(t) \in \mathrm{X}^j,\ u_{t_k}^j(t) \in \mathrm{U}^j; \tag{7d}$$

$$t \in [t_k, t_k + T]; (i,j) \in E$$

$$x_{t_k}^i(t_k + T) \in \mathrm{X}_f^i \tag{7e}$$

$$x_{t_k}^j(t_k + T) \in \mathrm{X}_f^j;\ (i,j) \in E$$

In Eq. (7), $J_T^i(t)$ comes from Eq. (4). Vectors X^i, U^i and X_f^i denote the set of admissible states, inputs and final states, respectively, for i^{th} vehicle. Signal $\tilde{u}_{t_k}^i(\cdot)$ denotes the trajectory of optimal inputs for all vehicles over $[t_k, t_k + T]$. The control action obtained by solving the optimization problem $P^i(t_k)$ is implemented during the *execution time* δ until the next update. Repeating this procedure online yields the closed-loop solution of RHC.

C. DRHC Algorithm

Each vehicle i at any sampling time sends its states to its neighboring vehicles. Furthermore, every vehicle i receives the information on states of its neighbors. Based on such information, each vehicle i solves the optimal problem $P^i(t_k)$ using Algorithm1:

Algorithm 1: At any time instant t_k, each vehicle i:

1) Let $k=0$
2) Send $x^i(t_k)$ to the neighboring vehicles and receive the most updated information from neighboring vehicles ($\hat{x}^j(t_k)$).
3) Solve $P^i(t_k)$ and generate the control action $u^i_{t_k}(\cdot)$ for $[t_k, t_k+T]$.
4) Execute the control action for individual vehicle i over the time interval $[t_k, t_{k+1}]$.
5) $k=k+1$. Goto step 2.

This algorithm is repeated until the assigned target (here origin) is reached. The targets are assumed to be known and assigned to each agent *a priori*.

D. Formation Cost

For the particular case of formation control, consider a group of mobile robots or flying vehicles that are required 1) to keep certain relative positions, and 2) to visit a set of targets. The decentralized individual and coupling cost functions for each vehicle are then defined as follows:

$$
\begin{aligned}
&L^i_T(x^i(t_k), u^i(t_k)) = \\
&\int_{t_k}^{t_k+T} \left(\left\|x^i_{t_k}(\tau)\right\|_Q^2 + \left\|u^i_{t_k}(\tau)\right\|_R^2\right) d\tau + \left\|x^i_{t_k}(t_k+T)\right\|_P^2 \\
&l^{i,j}_T(x^i(t_k), x^i(t_k)) = \int_{t_k}^{t_k+T} \left\|x^i_{t_k}(\tau) - x^j_{t_k}(\tau)\right\|_S^2 d\tau
\end{aligned}
\tag{8}
$$

where P, Q, R and S are positive definite symmetric matrix. As there is no non-convex coupling constraint, this cost function allows applying a relative position constraint among the vehicles. Such approach is used extensively in the literature [3, 4].

III. Stability Analysis

Each vehicle relies on models of its neighbors to predict their. Note that $x^{i,j}_{t_k}(t)$ is the state vector of i^{th} vehicle at time t, computed by j^{th} vehicle at time step t_k. Also, it is assumed that $x^i_{t_k}(t) = x^{i,i}_{t_k}(t)$.

Theorem 1 (Stability): Assume the matrix penalties P, Q, R and S are symmetric and positive definite in (8). Then, a sufficient condition for the asymptotic stability of DRHC problem $P^i(t_k)$ at the origin, with cost functions (8) is:

$$\varepsilon^i(t_k) \le \kappa^i(t_k) \tag{9}$$

where $\varepsilon^i(t_k)$ is the *prediction mismatch* of the optimization problem $P^i(t_k)$, over $[t_{k+1}, t_k+T]$, given as follows:

$$
\begin{aligned}
\varepsilon^i(t_k) = \sum_{j|(i,j)\in E} \int_{t_{k+1}}^{t_k+T} \Bigg[\left\|x^{j,j}_{t_k}(t) - x^{j,i}_{t_k}(t)\right\|_Q^2 \\
+ \left\|x^{j,j}_{t_k}(t) - x^{j,i}_{t_k}(t)\right\|_S^2 + \left\|u^{j,j}_{t_k}(t) - u^{j,i}_{t_k}(t)\right\|_R^2 \Bigg] dt
\end{aligned}
\tag{10}
$$

and the bound $\kappa^i(t_k)$ is given as:

$$
\begin{aligned}
\kappa^i(t_k) = \int_{t_k}^{t_{k+1}} \left(\left\|x^{i,i}_{t_k}(t)\right\|_Q^2 + \left\|u^{i,i}_{t_k}(t)\right\|_R^2\right) dt \\
+ \sum_{j|(i,j)\in E} \Bigg[\int_{t_k}^{t_{k+1}} \Big(\left\|x^{j,i}_{t_k}(t)\right\|_Q^2 + \left\|u^{j,i}_{t_k}(t)\right\|_R^2 \\
+ \left\|x^{i,i}_{t_k}(t) - x^{j,i}_{t_k}(t)\right\|_S^2 \Big) dt \Bigg]
\end{aligned}
\tag{11}
$$

Proof: The proof is removed due to page restriction.

Stability condition (9) implies a reduced prediction mismatch decreases the left- hand side of inequality (9) and eases satisfying the stability condition as opposed to a larger mismatch.

IV. Performance Analysis

For formation control, it is desired that vehicles keep certain relative positions. Hence, the decentralized performance metric is formulated as follows:

$$I^i(\tilde{x}^i(t_k)) = \sum_{j|(i,j)\in E} \int_{t_k}^{t_k+T} \left\|x^i(t) - x^j(t) - r^{ij}(t)\right\|_S^2 dt \tag{12}$$

where $r^{ij}(t)$ is the vector of desired relative positions between the i^{th} and the j^{th} vehicles. It is desired that $I^i(\tilde{x}^i(t_k)) = 0$. Any deviation from that will be studied using perturbation analysis as follows:

$$
\begin{aligned}
&x^i(t) \to x^i(t) + \Delta x^i(t) \\
&x^j(t) \to x^j(t) + \Delta x^j(t) \\
&I^i(\tilde{x}^i(t_k)) \to I^i(\tilde{x}^i(t_k)) + \Delta I^i(\tilde{x}^i(t_k))
\end{aligned}
\tag{13}
$$

substituting (13) in (12) and using triangular inequality of norms yield:

$$
\begin{aligned}
\Delta I^i(\tilde{x}^i(t_k)) \le \sum_{j|(i,j)\in E} \int_{t_k}^{t_k+T} \left\|\Delta x^i(t) - \Delta x^j(t)\right\|_S^2 dt = \\
\sum_{j|(i,j)\in E} \int_{t_k}^{t_k+T} \left\|[x^{i,i}_{t_k}(t) - x^{i,j}_{t_k}(t)] - [x^{j,j}_{t_k}(t) - x^{j,i}_{t_k}(t)]\right\|_S^2 dt \le
\end{aligned}
$$

$$\sum_{j|(i,j)\in E} \int_{t_k}^{t_k+T} \left(\left\|x_{t_k}^{i,i}(t)-x_{t_k}^{i,j}(t)\right\|_S^2+\left\|x_{t_k}^{j,j}(t)-x_{t_k}^{j,i}(t)\right\|_S^2\right)dt \quad (14)$$

Comparing the right-hand side of the above inequality with mismatch parameter (10) one can find similarities. Each term in right-hand side of (14) appears in the mismatch parameter of i^{th} and j^{th} agents, and is actually the mismatch in the states. However, the third term in mismatch parameter (10) which is the mismatch in input does not appear in right-hand side of (14). Since the mismatch in input can cause the state mismatch one can conclude that the right-hand side of (14) and (10) are equivalent in the sense that any change in the mismatch parameter (10) can change the right-hand side of (14) which is an upper bound on the error $\Delta I^i(\tilde{x}^i(t_k))$. This means the mismatch can increase the bound on error in $I^i(\tilde{x}^i(t_k))$ and lead to worse performance. This can be seen in simulations in Section VI (Figure 3). In fact, with a zero mismatch, considering (14) it follows that $\Delta I^i(\tilde{x}^i(t_k)) \to 0$.

V. Stability and Performance Enhancement Using Communication

We showed in Equations (9) and (14) that the mismatch parameter is a key parameter in the stability and performance properties of the DRHC architecture. Hence, the communication must be used in such a way as to reduce the mismatch parameter. Consequently, at any time instant based on the amount of mismatch parameter we can have a measure of the performance and stability of the entire fleet and efficiently distribute the available communication resources to achieve better stability and performance results. For instance, in the case of limited communication bandwidth, the higher portion of bandwidth will be employed to communicate with the agent(s) with larger mismatch. An agent is said to be in a critical situation if the stability of the system is in jeopardy according to (9).

However, one important problem is that even in the case of no communication delay at any time instant t_k, the corresponding mismatch is not available. One remedy to this is to use the mismatch from previous time steps or to use a bound on mismatch.

The following algorithm first finds the vehicles in a critical situation in the subgroups by measuring the mismatch, then, it distributes the available communications to improve the performance of the vehicles. τ denotes the communication delay.

Algorithm 2: At any time instant t_k, each vehicle *i*:

1. Communicate $\varepsilon^i(t_k)$ to neighboring vehicles.
2. Find q^{th} member in the set of neighbors so that: $\varepsilon^q = Max\{\varepsilon^j(t_{k-1}-\tau);(i,j)\in E\}$.
3. If $\varepsilon^q > \varepsilon_\circ$ then allocate the communication bandwidth considering that the q^{th} agent is in critical situation.
4. Follow Algorithm 1.

$\varepsilon_\circ$ is a design parameter and defines the desired upper bound on the mismatch. For the sake of stability it is required that $\varepsilon_0 \le \kappa^i(t_k)$ according to (9); and this must be taken into account. This algorithm is a modified version of Algorithm 1 while at every iteration, steps 1, 2 and 3 will be executed first to allocate the communication resources efficiently. The next section will demonstrate, via simulations, the 3rd step of the algorithm.

VI. Simulations

A formation of a fleet of miniature rotorcrafts with the 3DOF nonlinear dynamics is considered [12]. The main rotor and tail rotor thrusts are saturated at: $0 \le T_{mr} \le 1000$ and $0 \le T_{tr} \le 20$ where T_{mr} and T_{tr} are the main rotor and tail rotor thrust forces respectively. Also: $V_{\max} = 10\ m/\sec$ (*Velocity constraint*). The SNOPT optimization package [13] is used to solve the RHC problem. The actual trajectories for 6 vehicles in a triangular formation are shown in Figure 1. The corresponding distance history is depicted in Figure 2 for some typical scenario. In this formation, it is desired that moving vehicles keep a relative distance of 3m while flying in a triangular formation. As seen from Figure 2 the vehicles reach the desired distances after some time.

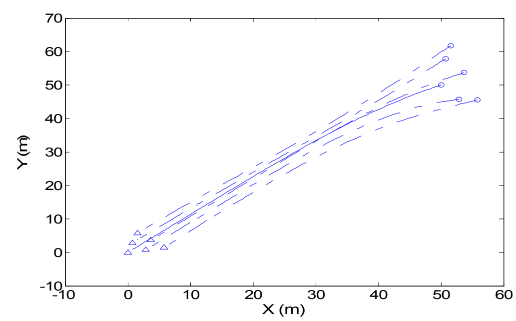

Figure 1. Triangular formation of a fleet of 6 vehicles.

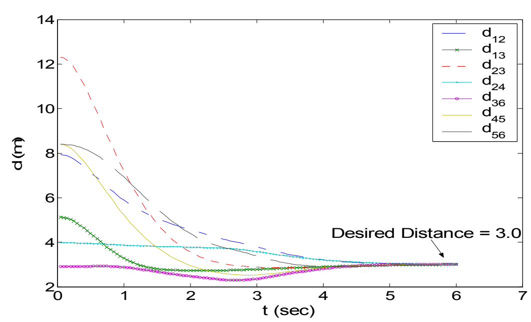

Figure 2. Relative distance profile in triangular formation

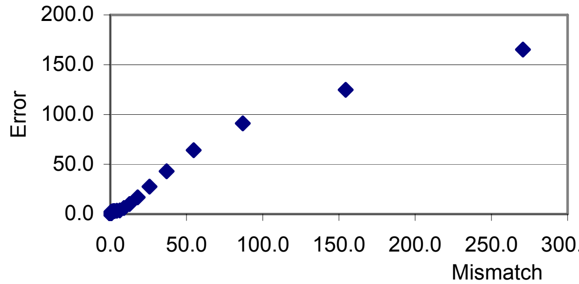

Figure 3. Error vs. Mismatch

A. Error (Performance) & Communication Rate & Communication Delay vs. Mismatch:

Figure 3 shows the maximum error in desired relative distance (12) versus mismatch (10) for different simulations. As seen from Figure 3 the error will increase with the mismatch. Such numerical result corroborates Equation (14).

Four different simulations are run with different sampling time (communication rate). As seen from Figure 4, a faster communication rate (smaller sampling time) results in a decrease in the mismatch. As another case study, the effect of communication delay on mismatch is investigated. Figure 5 shows the mismatch time history for 7 different simulations. The simulations differ only in communication delays. As seen from Figure 4 and Figure 5, the overall mismatch will increase with the communication delay and a higher sampling time. Consequently, from the stability and performance analysis results we can conclude that communication delay and slower communication rate can have an adverse effect on the stability and performance, which is intuitively expected.

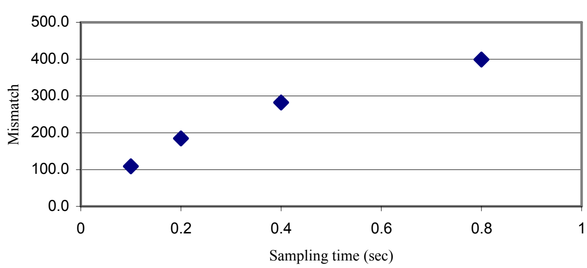

Figure 4. Mismatch vs. Communication rate

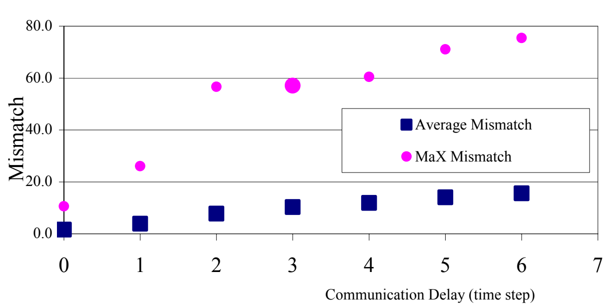

Figure 5. Mismatch vs. Communication Delays

B. Limited bandwidth Communication

In this subsection the proposed algorithm 2 is applied to the case where the communication bandwidth is limited. Consider a network of vehicles, where the communication channel of each vehicle is used to communicate with neighboring vehicles. Hence, in such situation, the following communication constraint must be satisfied by each vehicle i when communicating with neighbors:

$$\sum_{j|(i,j)\in E} \frac{K_i}{\tau_{ij}} \leq B_i \qquad (15)$$

where, τ_{ij} is the delay for transmitting the information form i to j. K_i is the size of i^{th} message (bits/sample) and B_i (bits/sec) is the bandwidth available with the communication channel of vehicle i. In normal condition when none of the neighbors of i^{th} vehicle are in critical situation, equal bandwidth portions will be allocated to all neighbors. However, in the emergency case where an agent q in the neighboring set of i^{th} vehicle, is in a critical situation, the neighboring vehicles of q assign more bandwidth for communicating with q. The communication delay in this case is calculated as follows:

$$\tau_{iq} = N_n^i \frac{K}{\eta B} \quad ; \quad q\,|\,(i,q)\in E \quad ; \quad 1<\eta \qquad (16)$$

where, η is a design parameter and defines the portion of bandwidth allocated to the q^{th} vehicle. Hence, considering (15) for the rest of neighboring vehicles of i, the delay is assigned as follows:

$$\tau_{ij} \geq \frac{K(N_n^i - 1)}{B(1-\frac{\eta}{N_n^i})} \quad ; j\,|\,(i,j)\in E \;\; , j\neq q \qquad (17)$$

This pattern will be used for the same scenario as in previous subsections. In the following simulations we assume $\frac{K}{B}=2$, and choose $\eta = 1.25$ and $\varepsilon_\circ = 100$. K is the size of messages and B comes from the capacity of communication channel. η and $\varepsilon_\circ$ are design parameters; η determines the portion of bandwidth allocated for communication with the agent in worse (or critical) situation and $\varepsilon_\circ$ must be chosen so that $\varepsilon_\circ \leq \kappa^i_{\min}(t)$ for the sake of stability according to (9).

Remark 1: As the agents move closer to their target, $\kappa^i(t)$ approaches zero, this can be seen from (11) and from the simulations. This means $\kappa^i_{\min}(t) \to 0$ which makes it difficult to choose an appropriate $\varepsilon_\circ$. To circumvent this problem, we neglected the steady-state response and chose $\kappa^i_{\min}(t)$ based on the transient response. A comprehensive investigation for choosing $\varepsilon_\circ$ and η is required.

The simulation results for two different cases are depicted in Figure 6 and Figure 7 for the formation flight of three vehicles. In Figure 6, the error parameter (12), corresponding to the second vehicle (the error profile for other vehicles follows the same pattern), is plotted versus time for two different cases. First, an equal bandwidth allocation strategy is utilized using Algorithm 1; the average error for this case is 225. Second, proposed Algorithm 2 allocates bandwidth so that the average error is reduced to 70. In this simulation any of the agents may be in the critical situation at any time but most of the time the second vehicle is in critical situation.

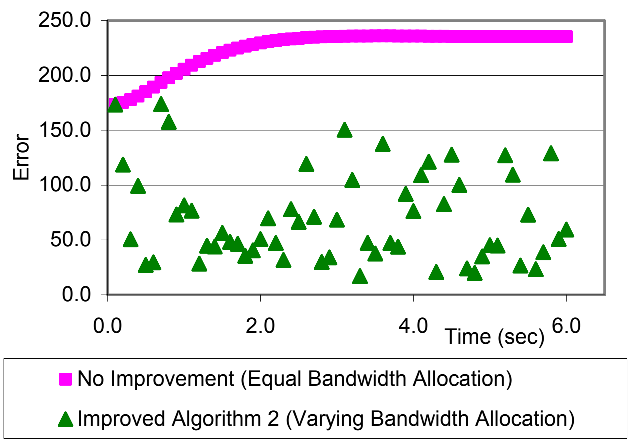

Figure 6: Error history corresponding to improved algorithm vs. algorithm1

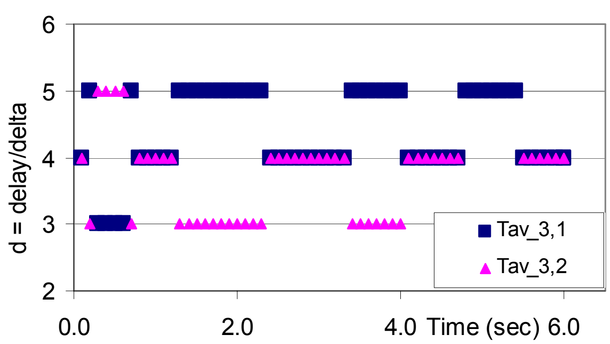

Figure 7: Delay variation in the channel of third vehicle using improved algorithm

The bandwidth allocation leads to varying communication delays for each vehicle as seen in Figure 7, where the time history of the delay allocation (due to bandwidth allocation) is plotted for the communication channel of the third vehicle. The communication delay is denoted by τ and $(d-1)\delta \le \tau \le d\delta$ where $d \in \mathbb{N}$. As seen from Figure 7 whenever there is no critical situation both the neighboring vehicles 1 and 2 are assigned the same communication delay, namely *d=4*. However, in the case of one agent in critical situation where the communication delay of one vehicle is reduced to *d=3*, the penalty is that the communication delay corresponding to the other neighbor will increase to *d=5* to satisfy the communication constraint (15).

VII. Conclusion

The results of analyzing the feasibility, stability and performance of DRHC imply that the mismatch between predicted and actual plans of each agent plays an important role in the stability and performance of the entire fleet. Based on this key result, a new improved algorithm for DRHC is proposed which leads to superior stability and performance of the team by communication bandwidth allocation.

References

[1] M.C De Gennaro and A. Jadbabaie, "Formation Control for a Cooperative Multi-Agent System using Decentralized Navigation Functions", *American Control Conference,* 2006, June 14-16, 2006, pp. 1346 – 1351.

[2] R. Franz , M. Milam and J. Hauser, "Applied Receding Horizon Control of the Caltech Ducted Fan," *IEEE ACC*, Anchorage, 2002.

[3] T. Keviczky , F. Borrelli and G. J. Balas, "Stability Analysis of Decentralized Receding Horizon Control for the decoupled systems ", *Proceedings of the 44th IEEE Conference on Decision and Control, and the European Control Conference 2005*, Seville, Spain, December 12-15, 2005, pp. 1689-1694.

[4] W. B. Dunbar and R. M. Murray, "Receding horizon control of multi-vehicle formations: A distributed implementation", Proceedings *of 43rd IEEE Conf. on Decision and Control*, 2004.

[5] A. Richards and J. How, "A decentralized algorithm for robust constrained model predictive control", *Proceedings of American Control Conference*, 2004.

[6] Y. Kuwata, A. Richards, T. Schouwenaars and J. How, "Decentralized Robust Receding Horizon Control for Multi-vehicle Guidance", *Proceedings of the 2006 American Control Conference,* Minneapolis, Minnesota, USA, June 14-16, 2006.

[7] Y. Kuwata, T. Schouwenaars, A. Richards, and J. How, "Robust Constrained Receding Horizon Control for Trajectory Planning" in *Proceedings of the AIAA Guidance, Navigation, and Control Conference*, August 2005.

[8] A. Richards and J. How, "Implementation of Robust Decentralized Model Predictive Control", *AIAA Guidance, Navigation and Control Conference,* 2005.

[9] L. Shi, C. Ko, Z. Jin, D. Gayme, V. Gupta, S. Waydo and R. M. Murray, "Decentralized Control across Bit-Limited Communication Channels: An Example", *2005 American Control Conference*, June 2005. Portland, OR, USA.

[10] P. E. Rybski, S. A. Stoeter, M. Gini, D. F. Hougen, N. Papanikolopoulos, "Effects of limited bandwidth communications channels on the control of multiple robots", Proceedings of 2001 IEEE/RSJ International Conference on Intelligent Robots and Systems, Maui, HI, USA, Oct. 2001.

[11] D. Q. Mayne, J. B. Rawlings, C. V. Rao and P. O. Scokaert., "Constrained model predictive control: Stability and optimality", *Automatica*, 36, 2000, pp. 789-814.

[12] V. Gavrilets, B. Mettler, E. Feron, "Dynamic Model for a Miniature Aerobatic Helicopter", MIT Internal Report.

[13] P. E. Gill, W. Murray and M. A. Saunders, "User's Guide for SNOPT Version 7: Software for Large-Scale Nonlinear Programming", Department of Mathematics University of California, San Diego, La Jolla, CA 92093-0112, USA, May 30, 2006.